ACS NANO
Cite This: *ACS Nano* XXXX, XXX, XXX−XXX
www.acsnano.org

Three-Dimensional Printed Poly(vinyl alcohol) Substrate with Controlled On-Demand Degradation for Transient Electronics

Jinsu Yoon,[†,⊥] Jungmin Han,[†,⊥] Bongsik Choi,[†] Yongwoo Lee,[†] Yeamin Kim,[†] Jinhee Park,[†] Meehyun Lim,[‡] Min-Ho Kang,[§] Dae Hwan Kim,[†] Dong Myong Kim,[†] Sungho Kim,[*,∥] and Sung-Jin Choi[*,†]

[†]School of Electrical Engineering, Kookmin University, Seoul 02707, Korea
[‡]Mechatronics R&D Center, Samsung Electronics, Gyeonggi-do 18448, Korea
[§]Department of Nano-process, National Nanofab Center (NNFC), Daejeon 34141, Korea
[∥]Department of Electrical Engineering, Sejong University, Seoul 05006, Korea

Supporting Information

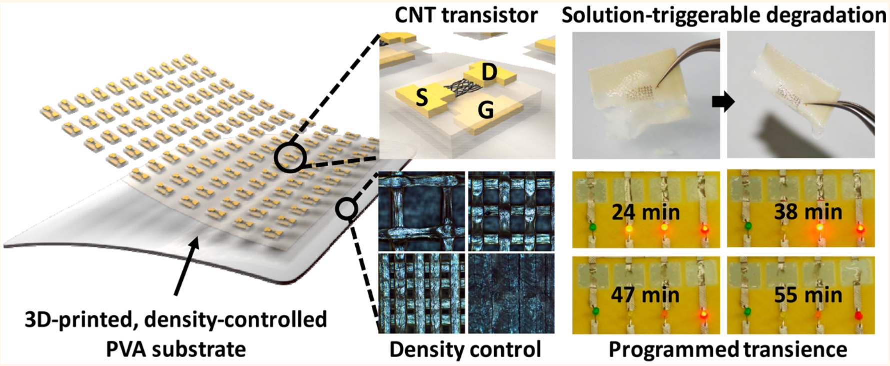

ABSTRACT: **Electronics that degrade after stable operation for a desired operating time, called transient electronics, are of great interest in many fields, including biomedical implants, secure memory devices, and environmental sensors. Thus, the development of transient materials is critical for the advancement of transient electronics and their applications. However, previous reports have mostly relied on achieving transience in aqueous solutions, where the transience time is largely predetermined based on the materials initially selected at the beginning of the fabrication. Therefore, accurate control of the transience time is difficult, thereby limiting their application. In this work, we demonstrate transient electronics based on a water-soluble poly(vinyl alcohol) (PVA) substrate on which carbon nanotube (CNT)-based field-effect transistors were fabricated. We regulated the structural parameters of the PVA substrate using a three-dimensional (3D) printer to accurately control and program the transience time of the PVA substrate in water. The 3D printing technology can produce complex objects directly, thus enabling the efficient fabrication of a transient substrate with a prescribed and controlled transience time. In addition, the 3D printer was used to develop a facile method for the selective and partial destruction of electronics.**

KEYWORDS: *three-dimensional printer, transient electronics, poly(vinyl alcohol), carbon nanotubes, network, transistor*

Durable and robust silicon-integrated circuits (ICs) have been developed over the last few decades and have been used in almost every aspect of daily life. Historically, engineering materials and designs have been emphasized that have been optimized for decades of reliable operation. Numerous works regarding the opposite behavior of traditional ICs have been published recently; namely, the devices not only stop functioning but also disintegrate completely in a well-defined, controlled short timeframe.[1−10] These applications are referred to as "transient electronics" and could probably be applied to a significant number of groundbreaking military applications; in the medical fields for diagnostics, treatment, and health monitoring as degradable environmental sensors; and in consumer electronics with fast-

Received: March 25, 2018
Accepted: May 23, 2018
Published: May 23, 2018

DOI: 10.1021/acsnano.8b02244
ACS Nano XXXX, XXX, XXX−XXX

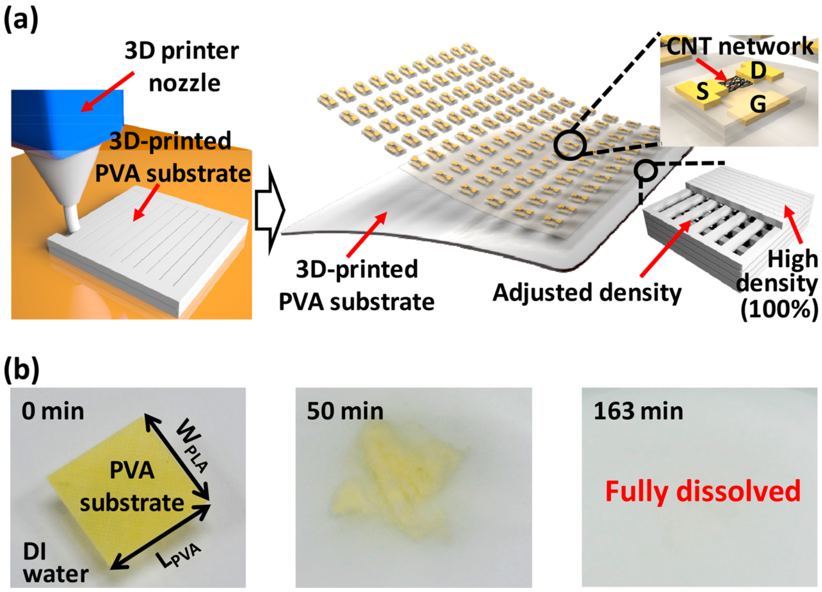

Figure 1. (a) Our concept of transient electronics based on a 3D-printed PVA substrate. The 3D printing process used to form the 3D-printed PVA substrate (left) and the CNT-based transistors transferred onto the substrate (right). The 3D-printed PVA substrate consists of two regions: a top layer with a PVA density of 100% and a layer with controlled densities. (b) Image showing the time sequence of the degradation of the 3D-printed PVA substrate in DI water.

growing waste streams.[9−19] In addition, transient electronics can provide many research opportunities for electronic materials, device designs, and fabrication technologies.

Transient electronic devices reported to date have largely been based on hydrolyzable thin inorganic materials, such as silicon nanomembrane semiconductors,[1,4] metal electrodes,[5,15,16] and dielectrics.[1,20] Several biodegradable polymer materials, such as polycaprolactone (PCL), poly(glycolic acid) (PGA), poly(lactic acid) (PLA), and poly(lactic-*co*-glycolic acid) (PLGA), have also been employed as possible substrates for transient electronic devices.[3,10,11,21−25] Previous research has worked to achieve transience with the devices submerged in a biofluid or aqueous solution; hence, the lifetime of the transient electronic system was controlled by the dissolution rate of the substrate materials determined during their initial fabrication.[1,20,26] Despite the significant progress made for such solution-based transient electronics, their applications may be extremely limited because the transience time cannot be precisely controlled and is difficult to program. Recently, stimuli-responsive materials have been reported to enable the implementation of transient electronics that can be triggered for degradation as an immediate response to a specific environmental stimulus.[27−29] Among them, light- and heat-triggered transient electronics that provide a versatile pathway for material selection have been proven to yield precise control over the life cycles of the transient devices and expand the versatility of transient devices beyond dissolution methods.[28,29] Nevertheless, it is still difficult to implement a partial triggering method in which only a portion of the electronics can be destroyed in response to a stimulus for a specific application.

Here, we demonstrate facile carbon nanotube (CNT)-based transient electronics with accurately controlled and programmed transience times; that is, the electronics operate for prescribed times and disappear rapidly at controlled rates. To avoid any complex fabrication processes, we utilized a three-dimensional (3D) printer to form a water-soluble poly(vinyl alcohol) (PVA) substrate with well-controlled, preprogrammed transience times. Using a 3D printer, the transience time and rate were tuned simply by modifying the structural parameters of the 3D-printed PVA substrate, including its length, width, thickness, and density, during the 3D printing process, which provides solution-based transient electronics with tailorable disintegration. In addition, we present a partial degradation technique where only designated areas of the substrate were destroyed within the prescribed transience time owing to the use of a 3D-printed, density-controlled PVA substrate. Our proposed scheme should be able to serve as a toolbox for producing solution-based transient electronics for numerous applications.

RESULTS AND DISCUSSION

Figure 1a shows a schematic of our proposed transient device. The local back-gate configuration was chosen to implement the transient electronic CNT-based devices, in which highly purified, solution-processed 99% semiconducting CNTs (purchased from NanoIntegris Inc., USA) were utilized to form the CNT-percolated network channel. The PVA layers used as the transient substrate were printed using a 3D printer (SPROUT single nozzle, Former's Farm Inc., Korea). The 3D-printed PVA substrate was highly water-soluble because it contained many hydroxyl groups.[30] The structural parameters of the PVA substrate, including the PVA densities (D_{PVA}), were adjusted using the 3D printer, providing accurate control of the transience time and rate. A top layer of the substrate was always printed with 100% PVA density during the 3D printing, that is, with no empty spaces between the printed PVA lines, because the surface of the 3D-printed PVA substrate, particularly those with low PVA densities, had significant roughness, which limited the reliability of the device fabrication on the substrate. However, the density of the remaining PVA substrate was adjusted to control the transience time and rate. Detailed information about the 3D printing process is provided in the Methods section. First, to confirm the water solubility of the 3D-printed PVA substrate, a substrate with a length (L_{PVA}) of

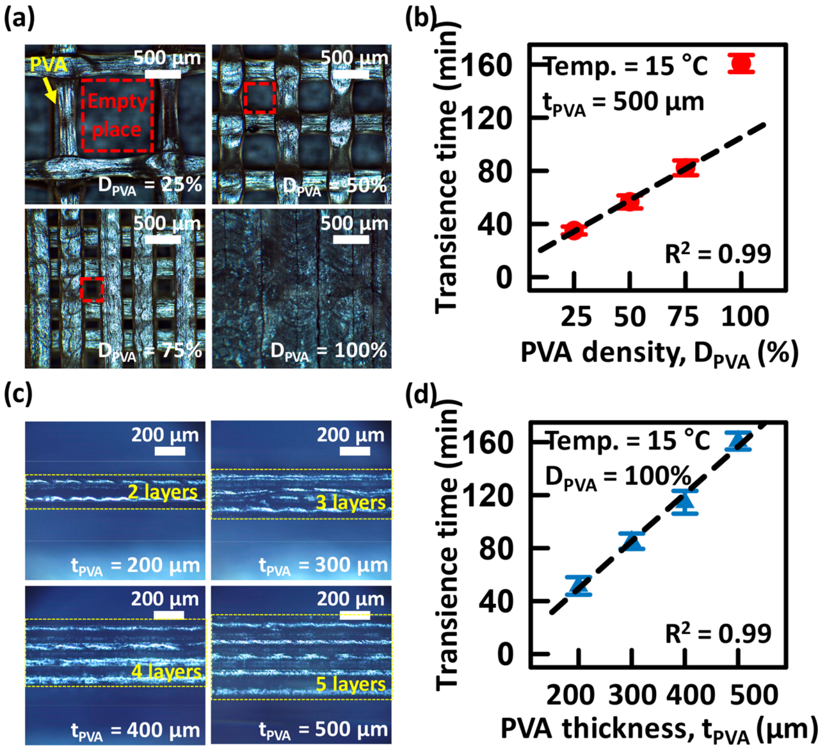

Figure 2. (a) Micrographs of the 3D-printed PVA substrate with various D_{PVA} values (25, 50, 75, and 100%). (b) Measured transience time of the 3D-printed PVA substrate density with various D_{PVA} values in DI water at 15 °C. The t_{PVA} is held at 500 μm. (c) Micrographs of the 3D-printed PVA substrate with various t_{PVA} values (200, 300, 400, and 500 μm). (d) Measured transience time of the 3D-printed PVA substrate density with various t_{PVA} values in DI water at 15 °C. The D_{PVA} is held at 100% (each error bar is based on five independent measurements).

2.4 cm, a width (W_{PVA}) of 2.4 cm, a thickness (t_{PVA}) of 500 μm, and D_{PVA} = 100% was placed in deionized (DI) water at 15 °C, as shown in Figure 1b. The 3D-printed PVA substrate in DI water initially floated and started to dissolve. Then, it slowly sank to the bottom of the water within 50 min. Finally, the PVA substrate disappeared within 163 min through simple dissolution, which indicates that modification of the 3D-printed PVA substrate is necessary to achieve more rapid degradation.

Theoretically, the transience time of the PVA substrate depends strongly on various parameters, such as the amount of solute (in this case, PVA), the surface area of the solute exposed to the solvent (in this case, DI water), and the temperature of the solvent. In most cases, the dissolution time can be decreased by reducing the amount of solute, increasing the surface area of the solute, and increasing the temperature of the solvent. Therefore, the transience time can be adjusted by modifying the structural parameters of the 3D-printed PVA substrate. First, to explore the controllability of the transience time, the PVA substrates were printed using a 3D printer by adjusting the D_{PVA} (*i.e.*, 25, 50, 75, and 100%) at a fixed substrate size (W_{PVA} = 2.4 cm, L_{PVA} = 2.4 cm, and t_{PVA} = 500 μm) and varying the t_{PVA} (*i.e.*, 200, 300, 400, and 500 μm) at a fixed D_{PVA} of 100%. Controlling D_{PVA} and t_{PVA} can be the most effective method to adjust the transience time because the top surface area of the substrate on which the devices were fabricated was left unchanged.

Figure 2a presents top-view micrographs of the 3D-printed PVA substrates with various values of D_{PVA} (25, 50, 75, and 100%). D_{PVA} was controlled during the 3D printing process by adjusting the size of the empty space between the printed, additive PVA lines. However, as noted above, the surface of the PVA substrate with low PVA densities was rough, thereby decreasing the reliability of the device fabrication. Therefore, the top layer of the PVA substrate was invariably printed with a PVA density of 100%. That is, the water-soluble, 3D-printed PVA substrate consisted of two regions: a top region with a fixed PVA density of 100% and a bottom region with variable PVA densities. The thicknesses of the top and bottom regions were approximately 100 and 400 μm, respectively, yielding a total thickness of approximately 500 μm. The measured transience time of the 3D-printed PVA substrates with different densities but the same substrate size (*i.e.*, the same L_{PVA} and W_{PVA}) clearly increased with D_{PVA}, as shown in Figure 2b. The transience time was defined as the time taken until the 3D-printed PVA substrate completely disappeared according to the naked eye. The transience time was decreased by approximately 400% as the D_{PVA} increased from 25 to 100%. The transience time increased linearly until the D_{PVA} reached 100%. This trend is attributed to the linear increase in the amount of PVA solute in the substrate for higher D_{PVA} values. However, an abrupt increase in the transience time was observed at a D_{PVA} of 100% because the water cannot easily penetrate inside of the 3D-printed PVA substrate. Furthermore, the t_{PVA} can also be an effective mediator of the transience behavior, so we evaluated the transience time for various t_{PVA} values. Figure 2c shows side views of the 3D-printed PVA substrates with different t_{PVA} values ranging from 200 to 500 μm. As the t_{PVA} increased from 200 to 500 μm, the dissolution of the substrates was delayed by 400% (Figure 2d). Moreover, the transience time linearly increased with t_{PVA}; hence, the transience time was highly predictable. The tendencies regarding the transience time of the 3D-printed PVA substrates with various D_{PVA} and t_{PVA} values are strongly correlated to the surface-to-volume ratio of the 3D-printed PVA substrate (Figures S1−S3). Furthermore, we

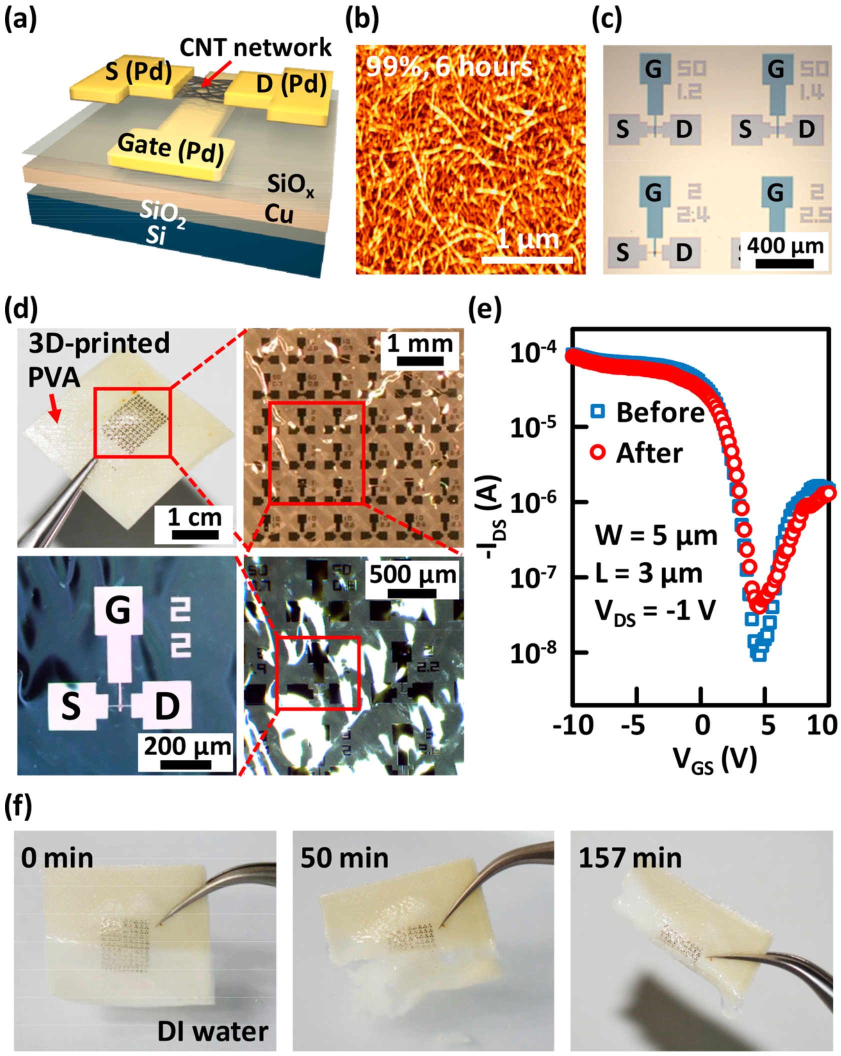

Figure 3. (a) Schematic of the fabricated CNT transistor on a rigid substrate before performing the transfer printing process. (b) AFM image (2.5 μm × 2.5 μm, z-scale is 10 nm) of the CNT-percolated network channel. (c) Optical micrograph of the CNT transistors fabricated on a rigid substrate. (d) Optical images of the CNT transistors transferred onto the 3D-printed PVA substrate. (e) Transfer curves (I_{DS}−V_{GS}) at V_{DS} = −1 V before (blue line) and after (red line) the transfer printing process. (f) Time sequences showing the destruction of the transient CNT transistors in DI water.

investigated the transience time of the 3D-printed PVA substrates while varying an environmental condition, such as the temperature of DI water. Figure S4 shows that the transience time of the 3D-printed PVA substrate was reduced as the temperature of the DI water increased because the water molecules became more active. This observation can be explained by the Arrhenius law, as the temperature dependence of the dissolution rate is generally known to follow the Arrhenius equation.[31] We confirmed that the transience time of the 3D-printed PVA substrate has an exponential dependence on the temperature of the DI water.

Destruction of electronic devices driven by disintegration of the 3D-printed PVA substrate in water was demonstrated using CNT-based transistors. The highly purified, 99% semiconducting CNT-percolated network-based transistors were fabricated on the 3D-printed PVA substrate to exhibit the applicability of transient electronics. The CNT transistors possess excellent material properties, including electrical and mechanical properties, thus minimizing the amount of material wasted at the beginning setup of the transient electronics and providing favorable mechanics and processing options for heterogeneous integration into flexible substrates.[32−36] The CNT transistors were fabricated on the 3D-printed PVA substrates *via* a water-assisted transfer printing technique.[37] During device fabrication, exposing the 3D-printed PVA substrates to water would cause the degradation of the substrate; thus, the processes should be performed carefully. Although we utilized CNT-based transistors for the transient electronics in this work, any type of device that can be transferred onto the substrate could be chosen, such as silicon-based electronic devices. Figure 3a illustrates a schematic of the CNT transistors on the rigid substrate before carrying out the transfer printing processes. Initially, a copper (Cu) layer with a thickness of 300 nm was deposited by evaporation onto the substrate, in which a 55 nm thick SiO_2 layer was thermally grown on the n^+-doped silicon. After that, a SiO_x layer with a thickness of 300 nm was deposited by plasma-enhanced chemical vapor deposition as a supporting substrate. We utilized the local back-gate configuration for the local modulation of the electrical channel potential in the CNT transistors. A palladium (Pd) layer was first evaporated and patterned to implement the local-gate configuration. Next, a 70 nm thick SiO_x layer was deposited as a

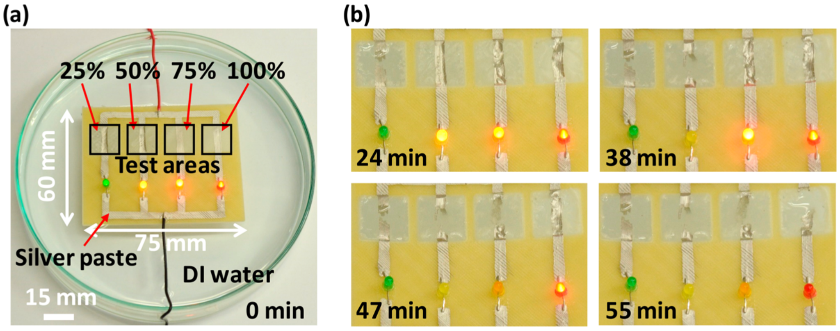

Figure 4. Application of the 3D-printed PVA substrate for multistage transition. (a) Experimental setup for a multistage transition where all LEDs were in the on state. (b) Time sequences showing that the LEDs were turned off according to the sequential destruction of the active areas with controlled D_{PVA} values.

gate dielectric. After that, an amine-terminated surface of the SiO_x layer was made with a 0.1 g/mL poly-L-lysine solution to effectively adhere the CNTs on the surface.[38] The CNT-percolated network as a channel was then formed by soaking the chip in 0.01 mg/mL 99% semiconducting CNT solution (purchased from NanoIntegris Inc.) and rinsing thoroughly with isopropyl alcohol and DI water. Afterward, titanium (Ti) and Pd layers (2 and 40 nm, respectively) were evaporated and patterned to form the source/drain electrodes. At the ends, photolithography and oxygen plasma steps were performed to remove the unwanted electrical pathways and isolate the devices from each other. Figure 3b shows an atomic force microscopy (AFM) image of a CNT-percolated network channel in the CNT transistors. The CNT-percolated networks were uniformly formed beyond a certain threshold at a given length, CNT density, and dimensions. Figure 3c illustrates a micrograph image of CNT transistors fabricated on a rigid substrate. Finally, the CNT transistors fabricated on a rigid substrate were transferred to the 3D-printed PVA substrate *via* a water-assisted transfer printing technique. At the end of the transfer processes, the thermal release tape (TRT) holding the CNT transistors was pasted onto the 3D-printed PVA substrate. The surface of the 3D-printed PVA substrate was preplanarized by applying DI water to the surface for a few seconds before the transfer printing processes. Although the top layer of the 3D-printed PVA substrate had a PVA density of 100%, the surface was not perfectly flat but actually rough; thus, a planarization step was necessary to achieve the stable transfer of the devices onto the 3D-printed PVA substrate (Figures S5 and S6). Finally, the TRT was detached from the structure at 100 °C to enable the fabrication of the transient CNT-based electronics on the 3D-printed PVA substrate. Figure 3d shows optical micrographs of the CNT transistors transferred to the 3D-printed PVA substrate.

The electrical properties of the CNT transistors before and after the transfer printing were investigated under ambient conditions, as shown in Figure 3e. The transfer curves (I_{DS}–V_{GS}; drain current *versus* gate voltage) of the CNT transistors were not significantly altered before and after the transfer printing processes, indicating that the CNT transistors were not damaged during the transfer printing. Figure 3f shows collected images in chronological order while the electronic devices driven by the disintegration of the 3D-printed PVA substrate at 15 °C DI water was destroyed. One-half of the 3D-printed PVA substrate onto which the CNT transistors were transferred was immersed in DI water to confirm the transient function by simple dissolution, as shown in Figure 3f. The 3D-printed PVA substrate slowly disappeared within the programmed time-frames, which were determined by the control of the PVA densities. This process causes the devices to physically disintegrate.

The partial degradation of the selected parts of the electronic components can be seen in the direction of current flow in the circuit or the geometry of the functional device and possibly alter or transform the functionality of the electronics. For previously reported transient systems that relied on the dissolution of components, selective or partial transience was difficult to design.[11] However, in this work, selective and partial destruction of electronic devices with prescribed and programmed transience times was simply achieved by controlling the D_{PVA} during the 3D printing process. First, the substrate with a length of 75 mm, a width of 60 mm, and a thickness of 1.6 mm was printed with a PVA density of 100%, except for the density-controlled active area. This active area, with a length of 15 mm and a width of 15 mm, was printed with different PVA densities (25, 50, 75, and 100%) for partial and selective destruction. As noted above, a top layer of the active area was printed with a PVA density of 100% for reliable device fabrication. The total thickness of the active area was 300 μm; the thicknesses of the top and bottom layers were 100 and 200 μm, respectively. To visually monitor the selective water-driven destruction of the 3D-printed PVA substrate, it was fabricated with four light-emitting diodes (LEDs) in parallel with silver (Ag) paste electrodes. The Ag electrodes were connected to green, yellow, orange, and red LEDs that were drawn on the active areas with various PVA densities, as shown in Figure 4a. The 3D-printed PVA substrate was soaked in DI water to evaluate the partial and selective degradation. After the substrate was soaked in DI water for 24 min, the first degradation was activated, and the Ag interconnection was destroyed by the dissolution of the PVA in the active area (D_{PVA} = 25%), resulting in the dimming of the green LED. After the substrate was soaked in DI water for 38 min, the second degradation was activated, and the yellow LED dimmed. After the substrate was soaked in DI water for 47 min, the third degradation was activated, and the orange LED dimmed. Finally, after the substrate was soaked in DI water for 55 min, all of the Ag interconnections with the LEDs were destroyed by the dissolution of the PVA at the active areas; that is, all LEDs were turned off, as shown in Figure 4b. The results show that the transience time of the 3D-printed PVA substrates can be controlled and programmed during 3D printing, which suggests the possibility of local selectivity for remapping the current flow

DOI: 10.1021/acsnano.8b02244

of a circuit and changing the functionality of electronic packages.

CONCLUSION

The transient system presented herein can guide the production of water-dissolvable electronic devices with the capacity to tailor the disintegration of electronic components. Using a 3D printer, we formed a water-soluble PVA substrate with tailored disintegration abilities. To obtain transient electronic devices, CNT-based transistors fabricated from a rigid substrate were then transferred onto the PVA substrate. The transience responses of the 3D-printed PVA substrate could be tuned, and a transience time-programmed multistage transition was demonstrated by altering the PVA densities in the substrate. Although we demonstrated only 3D-printed PVA as a transient substrate in this work, this method can be further expanded to other transition modes. The properties shown here may lead to the creation of a platform to develop devices that could effectively disappear or dispose of themselves on demand.

METHODS

Computer-Aided Design. Conventional 3D modeling software (Thinkercad, http://www.tinkercad.com) was utilized for designing the structures, and these were converted to gcode files for 3D printing using Cura (version 15.04).

3D Printing Process. The 3D printing was performed using a 3D printer (SPROUT single nozzle, Former's Farm Inc., Korea) based on fused deposition modeling.[17] Using only a computer-aided design file, we fabricated the PVA substrate by linking it with the 3D printer software. The designed substrate was then printed through a heated nozzle layer-by-layer using the PVA filament. In our experiment, the diameter of the 3D printing nozzle was 400 μm; the temperature was 190 °C; the nozzle moving speed was 10 mm/s, and the layer thickness was 100 μm. The entire printing process took less than 10 min for the 3D-printed PVA substrate with five layers at $D_{\mathrm{PVA}} = 100\%$, $W_{\mathrm{PVA}} = 2.4$ cm, and $L_{\mathrm{PVA}} = 2.4$ cm.

Water-Assisted Transfer Printing Technique. First, a TRT was attached to the CNT transistors fabricated on the rigid substrate. Next, the entire structure was immersed in DI water, and the TRT was carefully peeled off to begin to make water penetration between the Cu layer and SiO_2 layer. Then, the TRT holding the CNT transistors was detached from the rigid substrate in DI water. After that, the Cu layer on the backside of the detached structure was dissolved using a Cu etchant ($FeCl_3$). Subsequently, the TRT holding the structure was pasted onto the 3D-printed PVA substrate. At the ends, the TRT was peeled off from the structure *via* heating at 100 °C for several minutes.

Characterization of the CNT Transistors. The morphologies of the CNT network were evaluated by AFM (Park Systems, model XE-100). The CNT transistors were electrically characterized using a parameter analyzer (Agilent, 4156C).

Characterization of the Planarized Surface of the 3D-Printed PVA Surface. The surfaces of the 3D-printed PVA substrates were characterized using an optical surface profiler (NanoFocus, model μ-Surf) before and after being immersed in DI water.

ASSOCIATED CONTENT

Ⓢ Supporting Information

The Supporting Information is available free of charge on the ACS Publications website at DOI: 10.1021/acsnano.8b02244.

> Additional discussion about the calculation of the surface-to-volume ratio of the 3D-printed substrate, transience times with various DI water temperatures, and planarization of the surface of the 3D-printed PVA substrate using DI water (PDF)

AUTHOR INFORMATION

Corresponding Authors

*E-mail: sungho85kim@sejong.ac.kr.
*E-mail: sjchoiee@kookmin.ac.kr.

ORCID

Sung-Jin Choi: 0000-0003-1301-2847

Author Contributions

$^{\perp}$J.Y. and J.H. contributed equally to this work.

Notes

The authors declare no competing financial interest.

ACKNOWLEDGMENTS

This work was supported by the National Research Foundation (NRF) of Korea under Grant Nos. 2016R1A2B4011366 and 2016R1A5A1012966 and by the Future Semiconductor Device Technology Development Program (Grant No. 10067739) funded by the Ministry of Trade, Industry & Energy (MOTIE) and the Korea Semiconductor Research Consortium (KSRC).

REFERENCES

(1) Hwang, S.-W.; Tao, H.; Kim, D.-H.; Cheng, H.; Song, J.-K.; Rill, E.; Brenckle, M. A.; Panilaitis, B.; Won, S. M.; Kim, Y.-S.; Song, Y. M.; Yu, K. J.; Ameen, A.; Li, R.; Su, Y.; Yang, M.; Kaplan, D. L.; Zakin, M. R.; Slepian, M. J.; Huang, Y.; et al. A Physically Transient Form of Silicon Electronics. *Science* **2012**, *337*, 1640−1644.

(2) Kim, D.-H.; Kim, Y.-S.; Amsden, J.; Panilaitis, B.; Kaplan, D. L.; Omenetto, F. G.; Zakin, M. R.; Rogers, J. A. Silicon Electronics on Silk as a Path to Bioresorbable, Implantable Devices. *Appl. Phys. Lett.* **2009**, *95*, 133701.

(3) Bettinger, B. C. J.; Bao, Z. Organic Thin-Film Transistors Fabricated on Resorbable Biomaterial Substrates. *Adv. Mater.* **2010**, *22*, 651−655.

(4) Hwang, S.-W.; Park, G.; Edwards, C.; Corbin, E. A.; Kang, S.-K.; Cheng, H.; Song, J.-K.; Kim, J.-H.; Yu, S.; Ng, J.; Lee, J. E.; Kim, J.; Yee, C.; Bhaduri, B.; Su, Y.; Omennetto, F. G.; Huang, Y.; Bashir, R.; Goddard, L.; Popescu, G.; et al. Dissolution Chemistry and Biocompatibility of Single-Crystalline Silicon Nanomembranes and Associated Materials for Transient Electronics. *ACS Nano* **2014**, *8*, 5843−5851.

(5) Yin, L.; Cheng, H.; Mao, S.; Haasch, R.; Liu, Y.; Xie, X.; Hwang, S.-W.; Jain, H.; Kang, S.-K.; Su, Y.; Li, R.; Huang, Y.; Rogers, J. A. Dissolvable Metals for Transient Electronics. *Adv. Funct. Mater.* **2014**, *24*, 645−658.

(6) Guo, J.; Liu, J.; Yang, B.; Zhan, G.; Kang, X.; Tian, H.; Tang, L.; Chen, X.; Yang, C. Low-Voltage Transient/Biodegradable Transistors Based on Free-Standing Sodium Alginate Membranes. *IEEE Electron Device Lett.* **2015**, *36*, 576−578.

(7) Dagdeviren, C.; Hwang, S.-W.; Su, Y.; Kim, S.; Cheng, H.; Gur, O.; Haney, R.; Omenetto, F. G.; Huang, Y.; Rogers, J. A. Transient, Biocompatible Electronics and Energy Harvesters Based on ZnO. *Small* **2013**, *9*, 3398−3404.

(8) Kang, S.-K.; Hwang, S.-W.; Yu, S.; Seo, J.-H.; Corbin, E. A.; Shin, J.; Wie, D. S.; Bashir, R.; Ma, Z.; Rogers, J. A. Biodegradable Thin Metal Foils and Spin-On Glass Materials for Transient Electronics. *Adv. Funct. Mater.* **2015**, *25*, 1789−1797.

(9) Yoon, J.; Lee, J.; Choi, B.; Lee, D.; Kim, D. H.; Kim, D. M.; Moon, D.-I.; Lim, M.; Kim, S.; Choi, S.-J. Flammable Carbon Nanotube Transistors on a Nitrocellulose Paper Substrate for Transient Electronics. *Nano Res.* **2017**, *10*, 87−96.

(10) Hwang, S.-W.; Song, J.-K.; Huang, X.; Cheng, H.; Kang, S.-K.; Kim, B. H.; Kim, J.-H.; Yu, S.; Huang, Y.; Rogers, J. A. High-Performance Biodegradable/Transient Electronics on Biodegradable Polymers. *Adv. Mater.* **2014**, *26*, 3905−3911.

(11) Hwang, S.-W.; Kang, S.-K.; Huang, X.; Brenckle, M. A.; Omenetto, F. G.; Rogers, J. A. Materials for Programmed, Functional

Transformation in Transient Electronic Systems. *Adv. Mater.* **2015**, *27*, 47−52.

(12) Brenckle, M. A.; Cheng, H.; Hwang, S.; Tao, H.; Paquette, M.; Kaplan, D. L.; Rogers, J. A.; Huang, Y.; Omenetto, F. G. Modulated Degradation of Transient Electronic Devices Through Multilayer Silk Fibroin Pockets. *ACS Appl. Mater. Interfaces* **2015**, *7*, 19870−19875.

(13) Kim, D.-H.; Viventi, J.; Amsden, J. J.; Xiao, J.; Vigeland, L.; Kim, Y.-S.; Blanco, J. A.; Panilaitis, B.; Frechette, E. S.; Contreras, D.; Kaplan, D. L.; Omenetto, F. G.; Huang, Y.; Hwang, K.-C.; Zakin, M. R.; Litt, B.; Rogers, J. A. Dissolvable Films of Silk Fibroin for Ultrathin Conformal Bio-Integrated Electronics. *Nat. Mater.* **2010**, *9*, 511−517.

(14) Mannoor, M. S.; Tao, H.; Clayton, J. D.; Sengupta, A.; Kaplan, D. L.; Naik, R. R.; Verma, N.; Omenetto, F. G.; McAlpine, M. C. Graphene-Based Wireless Bacteria Detection on Tooth Enamel. *Nat. Commun.* **2012**, *3*, 763.

(15) Fu, K. K.; Wang, Z.; Dai, J.; Carter, M.; Hu, L. Transient Electronics: Materials and Devices. *Chem. Mater.* **2016**, *28*, 3527−3539.

(16) Jin, S. H.; Shin, J.; Cho, I.-T.; Han, S. Y.; Lee, D. J.; Lee, C. H.; Lee, J.-H.; Rogers, J. A. Solution-Processed Single-Walled Carbon Nanotube Field Effect Transistors and Bootstrapped Inverters for Disintegratable, Transient Electronics. *Appl. Phys. Lett.* **2014**, *105*, 013506.

(17) Zhu, B.; Wang, H.; Leow, W. R.; Cai, Y.; Loh, X. J.; Han, M.-Y.; Chen, X. Silk Fibroin for Flexible Electronic Devices. *Adv. Mater.* **2016**, *28*, 4250−4265.

(18) Yu, K. J.; Kuzum, D.; Hwang, S.-W.; Kim, B. H.; Juul, H.; Kim, N. H.; Won, S. M.; Chiang, K.; Trumpis, M.; Richardson, A. G.; Cheng, H.; Fang, H.; Thompson, M.; Bink, H.; Talos, D.; Seo, K. J.; Lee, H. N.; Kang, S.-K.; Kim, J.-H.; Lee, J. Y.; et al. Bioresorbable Silicon Electronics for Transient Spatiotemporal Mapping of Electrical Activity from the Cerebral Cortex. *Nat. Mater.* **2016**, *15*, 782−791.

(19) Hwang, S.-W.; Lee, C. H.; Cheng, H.; Jeong, J.-W.; Kang, S.-K.; Kim, J.-H.; Shin, J.; Yang, J.; Liu, Z.; Ameer, G. A.; Huang, Y.; Rogers, J. A. Biodegradable Elastomers and Silicon Nanomembranes/Nanoribbons for Stretchable, Transient Electronics, and Biosensors. *Nano Lett.* **2015**, *15*, 2801−2808.

(20) Kang, S.-K.; Hwang, S.-W.; Cheng, H.; Yu, S.; Kim, B. H.; Kim, J.-H.; Huang, Y.; Rogers, J. A. Dissolution Behaviors and Applications of Silicon Oxides and Nitrides in Transient Electronics. *Adv. Funct. Mater.* **2014**, *24*, 4427−4434.

(21) Lam, C. X. F.; Savalani, M. M.; Teoh, S.-H.; Hutmacher, D. W. Dynamics of *in Vitro* Polymer Degradation of Polycaprolactone-Based Scaffolds: Accelerated *Versus* Simulated Physiological Conditions. *Biomed. Mater.* **2008**, *3*, 034108.

(22) Woodruff, M. A.; Hutmacher, D. W. The Return of a Forgotten Polymer—Polycaprolactone in the 21st Century. *Prog. Polym. Sci.* **2010**, *35*, 1217−1256.

(23) Sabir, M. I.; Xu, X.; Li, L. A Review on Biodegradable Polymeric Materials for Bone Tissue Engineering Applications. *J. Mater. Sci.* **2009**, *44*, 5713−5724.

(24) Chiu, L. K.; Chiu, W. J.; Cheng, Y.-L. Effects of Polymer Degradation on Drug Released — Mechanistic Study of Morphology and Transport Properties in 50:50 Poly(dl-Lactide-Co-Glycolide). *Int. J. Pharm.* **1995**, *126*, 169−178.

(25) Huang, X.; Liu, Y.; Hwang, S.-W.; Kang, S.-K.; Patnaik, D.; Cortes, J. F.; Rogers, J. A. Biodegradable Materials for Multilayer Transient Printed Circuit Boards. *Adv. Mater.* **2014**, *26*, 7371−7377.

(26) Acar, H.; Cinar, S.; Thunga, M.; Kessler, M. R.; Hashemi, N.; Montazami, R. Study of Physically Transient Insulating Materials as a Potential Platform for Transient Electronics and Bioelectronics. *Adv. Funct. Mater.* **2014**, *24*, 4135−4143.

(27) Kaitz, J. A.; Diesendruck, C. E.; Moore, J. S. End Group Characterization of Poly(phthalaldehyde): Surprising Discovery of a Reversible, Cationic Macrocyclization Mechanism. *J. Am. Chem. Soc.* **2013**, *135*, 12755−12761.

(28) Hernandez, H. L.; Kang, S.-K.; Lee, O. P.; Hwang, S.-W.; Kaitz, J. A.; Inci, B.; Park, C. W.; Chung, S.; Sottos, N. R.; Moore, J. S.; Rogers, J. A.; White, S. R. Triggered Transience of Metastable Poly(phthalaldehyde) for Transient Electronics. *Adv. Mater.* **2014**, *26*, 7637−7642.

(29) Park, C. W.; Kang, S.-K.; Hernandez, H. L.; Kaitz, J. A.; Wie, D. S.; Shin, J.; Lee, O. P.; Sottos, N. R.; Moore, J. S.; Rogers, J. A.; White, S. R. Thermally Triggered Degradation of Transient Electronic Devices. *Adv. Mater.* **2015**, *27*, 3783−3788.

(30) Liang, J.; Huang, Y.; Zhang, L.; Wang, Y.; Ma, Y.; Guo, T.; Chen, Y. Molecular-Level Dispersion of Graphene into Poly(vinyl alcohol) and Effective Reinforcement of Their Nanocomposites. *Adv. Funct. Mater.* **2009**, *19*, 2297−2302.

(31) Ganor, J.; Mogollón, J. L.; Lasaga, A. C. The Effect of pH on Kaolinite Dissolution Rates and on Activation Energy. *Geochim. Cosmochim. Acta* **1995**, *59*, 1037−1052.

(32) Wang, C.; Chien, J.-C.; Takei, K.; Takahashi, T.; Nah, J.; Niknejad, A. M.; Javey, A. Extremely Bendable, High-Performance Integrated Circuits Using Semiconducting Carbon Nanotube Networks for Digital, Analog, and Radio-Frequency Applications. *Nano Lett.* **2012**, *12*, 1527−1533.

(33) Cao, Q.; Kim, H.-S.; Pimparkar, N.; Kulkarni, J. P.; Wang, C.; Shim, M.; Roy, K.; Alam, M.; Rogers, J. A. Medium-Scale Carbon Nanotube Thin-Film Integrated Circuits on Flexible Plastic Substrates. *Nature* **2008**, *454*, 495−500.

(34) Cao, Q.; Rogers, J. A. Ultrathin Films of Single-Walled Carbon Nanotubes for Electronics and Sensors: A Review of Fundamental and Applied Aspects. *Adv. Mater.* **2009**, *21*, 29−53.

(35) Zhang, J.; Wang, C.; Zhou, C. Rigid/Flexible Transparent Electronics Based on Separated Carbon Nanotube Thin-Film Transistors and Their Application in Display Electronics. *ACS Nano* **2012**, *6*, 7412−7419.

(36) Javey, A.; Guo, J.; Wang, Q.; Lundstrom, M.; Dai, H. Ballistic Carbon Nanotube Field-Effect Transistors. *Nature* **2003**, *424*, 654−657.

(37) Lee, C. H.; Kim, D. R.; Zheng, X. Fabrication of Nanowire Electronics on Nonconventional Substrates by Water-Assisted Transfer Printing Method. *Nano Lett.* **2011**, *11*, 3435−3439.

(38) Wang, C.; Zhang, J.; Ryu, K.; Badmaev, A.; De Arco, L. G.; Zhou, C. Wafer-Scale Fabrication of Separated Carbon Nanotube Thin-Film Transistors for Display Applications. *Nano Lett.* **2009**, *9*, 4285−4291.

DOI: 10.1021/acsnano.8b02244
ACS Nano XXXX, XXX, XXX−XXX